

HIGHLY SIDEROPHILE ELEMENTS IN PALLASITES AND DIOGENITES, INCLUDING THE NEW PALLASITE, CMS 04071. L. R. Danielson¹, M. Humayun², and K. Righter¹. ¹Mail Code KT, NASA JSC, 2101 NASA Rd 1, Houston, TX 77058. E-mail: ldaniels@ems.jsc.nasa.gov. ²National High Magnetic Field Laboratory and Dept. of Geological Sciences, Florida State University, Tallahassee, FL 32310.

Introduction: Pallasites are long thought to represent a metallic core-silicate mantle boundary, where the IIIAB irons are linked to the crystallization history of the metallic fraction, and the HED meteorites may be linked to the silicate fraction [1,2,3]. However, measurement of trace elements in individual metallic and silicate phases is necessary in order to fully understand the petrogenetic history of pallasites, as well as any magmatic processes which may link pallasites to both IIIAB irons and HED meteorites. In order to achieve this objective, abundances of a suite of elements were measured, including the highly siderophile elements (HSEs), in kamacite, taenite, troilite, schreibersite, chromite and olivine for the pallasites Admire, Imilac, Springwater, CMS 04071 (Figure 1). In the diogenites GRO 95555, LAP 91900, and MET 00436, metal, sulfide, spinel, pyroxene, and silica were individually measured.

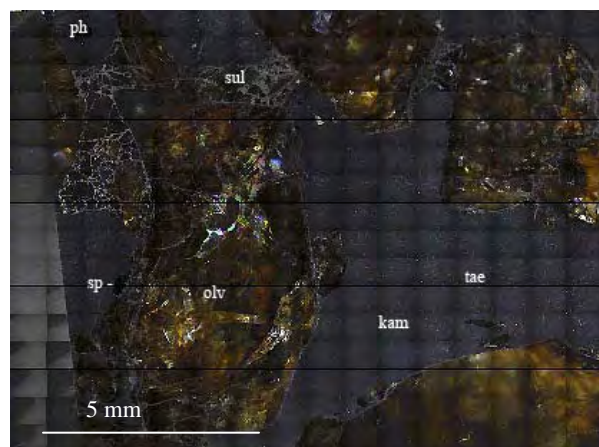


Figure 1. Reflected light image of CMS 04071. Phases are labeled in white, ph = phosphide (schreibersite), sp = chromite, olv = olivine, kam = kamacite, tae = taenite.

Analytical: Trace element microanalysis was performed using a CETAC LSX-200 laser ablation system coupled to a Finnigan ElementTM at the NHMFL, FSU, following procedures modified from Campbell and Humayun [4]. Elemental abundances were determined in line scan and spot mode, from the isotopes: ⁵³Cr, ⁵⁷Fe, ⁵⁹Co, ⁶⁰Ni, ⁶³Cu, ⁶⁹Ga, ⁷⁴Ge, ⁷⁵As, ⁹⁵Mo, ¹⁰²Ru, ¹⁰³Rh, ¹⁰⁵Pd, ¹⁸⁴W, ¹⁸⁵Re, ¹⁹²Os, ¹⁹³Ir, ¹⁹⁵Pt, and ¹⁹⁷Au. Ablated tracks across individual mineral grains ranged from 100 μ m to 2.36 mm long, and 30 to 110 μ m

wide; spots were 65 and 80 μ m in diameter, depending on the grain size. Standards were Filomena, Hoba and SRM-612.

Major elements were characterized using the Cameca SX100 at NASA JSC, with a 15kV accelerating voltage and 20 μ A sample current.

Results: Some zoning was noted at phase boundaries, so partition coefficients (D) were extracted by using average values of elements for flat portions of each traverse and using spot analyses. For Imilac, $D(\text{Os,Re,Ru,Pt,Rh})_{\text{taenite/kamacite}}$ range from 1.0 to 1.7, while Au, Pd, Cr, Co, As, and W partitioned preferentially into kamacite (Figure 2). However, for CMS 04071, $D(\text{Os,Re,Pt})_{\text{taenite/kamacite}}$ are < 1 . $D(\text{HSE})_{\text{metal/troilite}}$ for Imilac, Admire, and Springwater ranged from ~ 1 to 100. Cr, Cu, Co, As and Re partitioned preferentially into troilite. Metal-sulfide partitioning experiments by [5] agree with the results for Cr, Cu, and As, for $D_{\text{metal/sulfide}} < 1$, but not Re, which is expected to be > 1 . Ge, Au, and Pd, were found to be chalcophile in partitioning experiments, but not in the pallasite system. Relative to CI chondrite, metals follow a pattern of Pt-Ir $<$ Ru-Rh-Au-Pd for Imilac, Springwater, and Admire, while CMS 04071 follows the reverse.

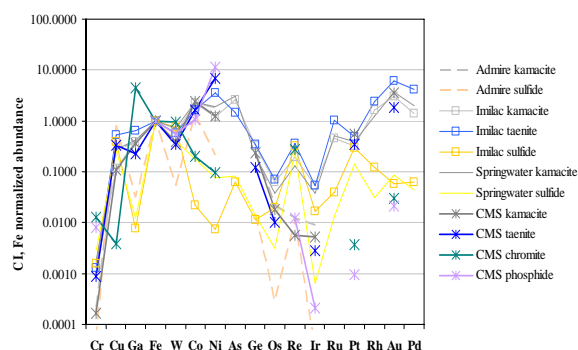


Figure 2. Chondrite and Fe normalized elements in order of increasing volatility.

$D(\text{HSE})_{\text{taenite/kamacite}}$ for Imilac is in good agreement with previous studies for Brenham, IAB and IIIAB irons, in which D's cluster around 1.5 [6,7], though $D(\text{HSE})_{\text{taenite/kamacite}}$ for CMS 04071 is lower than these irons. $D(\text{Re,Os})_{\text{metal/troilite}}$ are several orders of magnitude less than the 10^3 - 10^4 for IAB irons [8].

$D(\text{HSE})_{\text{metal/ol}}$ is comparable to values reported by [9], except for Re and Ir which are $< 10^4$ (Figure 3). A relatively large $D(\text{Ge})_{\text{metal/olv}}$ of $10^4 - 10^5$ agrees with previous studies [10,11]

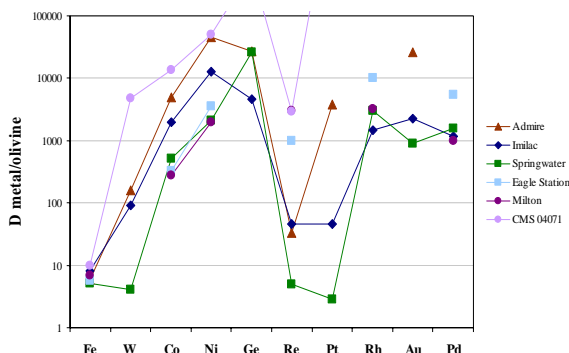


Figure 3. $D_{\text{metal/olivine}}$ for pallasites. Eagle Station and Milton are from [9]. $D(\text{Ge}, \text{Pt})_{\text{metal/ol}}$ for CMS 04071 is $> 10^5$.

CMS 04071. Complex phases have been identified in this meteorite. Olivines of $\text{Fa}_{11.8}$ are rounded and rimmed by an Fe-rich phase (Figure 5), which also commonly contains chromites. Schreibersite commonly occurs as an Ni-rich quench phase associated with kamacite – taenite, and larger, Fe-rich regions associated with sulfide.

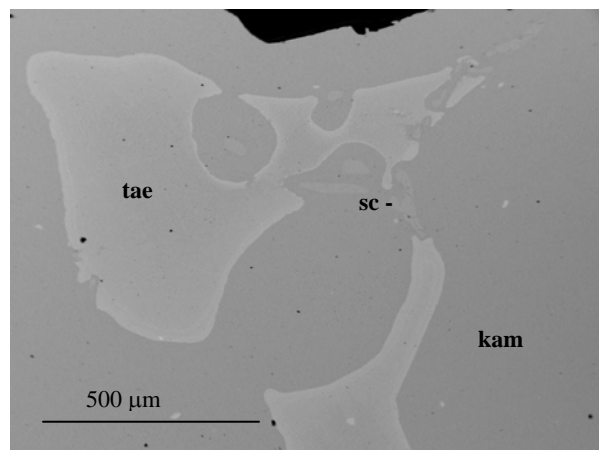


Figure 5. BSE image of metal region in CMS 04071. Abbreviations are kamacite – kam, taenite – tae, the Ni-rich schreibersite – sc.

Discussion and Conclusions: Fractionation of the HSEs in the pallasite metallic fraction was modeled using a IIIAB parent composition. An Imilac residual metal composition can be produced from 55% crystallization of a core, with increasing $D(\text{HSE})_{\text{solid metal/liquid metal}}$ from $X_S = 0$ to 0.1 [5]. For Imilac, these data are consistent with the metallic fraction derived from a late-stage residual metallic liquid from fractional crys-

tallization of a IIIAB metallic core. However, the crystallization history of the metal for the other pallasites is more complex, particularly CMS 04071, which contains 5 metallic phases.

The zoning (e.g., Cr, Cu, W, Re) across multiple phases in metals may be the result of diffusion on quench or post quench magmatic interaction.

In olivines, HSE abundances may be a product of metal inclusions, though if this is the case, it is unknown whether these inclusions represent a reaction product of the olivines, a trapped phase from the olivine cumulate magma, or a contaminant from the pallasite metal (as in *Santa Rosalia*, [13]).

Closure temperatures for these pallasites were calculated to be 800 to 1000 °C for Imilac and CMS 04071, comparable to 700 - 1000 °C calculated by [14]. However, an unreasonably high closure temperature of > 1800 °C was calculated for Admire and Springwater.

CMS 04071 can be classified using the scheme of [3] as, pallasite main group, anomalous metal (PMG-am) because of its high Au and Ge abundances.

References: [1] Scott, 1977, *Geochim. Cosmochim. Acta*, 41: 349-360. [2] Mittlefehldt et al., 1998, In: *Planetary Materials*, Papike J.J. (Ed), p. 195. [3] Wasson and Choi, 2003, *Geochim. Cosmochim. Acta*, 67: 3079-3096. [4] Campbell and Humayun, 1999, *Anal. Chem.*, 71: 939-946. [5] Chabot, 2004, *Geochim. Cosmochim. Acta*, 68: 3607-3618. [6] Hsu et al., 2000, *Geochim. Cosmochim. Acta*, 64: 1133-1147. [7] Hirata and Nesbitt, 1997, *Earth. Planet. Sci. Lett.*, 147: 11-24. [8] Shen et al., 1996, *Geochim. Cosmochim. Acta*, 60: 2887-2900. [9] Hillebrand et al., 2004, *LPSC XXXV*, No. 1278. [10] Schmitt et al., 1989, *Geochim. Cosmochim. Acta*, 53: 173-185. [11] Capobianco and Watson, 1982, *Geochim. Cosmochim. Acta*, 46: 235-240. [12] Buseck, 1977, *Geochim. Cosmochim. Acta*, 41: 717-740. [14] Seifert et al., 1988, *Geochim. Cosmochim. Acta*, 52: 603-616.